Available online at www.sciencedirect.com
SCIENCE DIRECT®
Journal of Hydrology 291 (2004) 254–277
Journal of Hydrology
www.elsevier.com/locate/jhydrol

Constraining dynamic TOPMODEL responses for imprecise water table information using fuzzy rule based performance measures

J.E. Freer[a,*], H. McMillan[b], J.J. McDonnell[c], K.J. Beven[a]

[a]*Department of Environmental Sciences, Lancaster University, IENS, Bailrigg, Lancaster, LA1 4YQ, UK*
[b]*Department of Geography, University of Cambridge, Downing Place, Cambridge, CB2 3EN, UK*
[c]*Department of Forest Engineering, 015 Peavy Hall, Oregon State University, Corvallis, OR 97331-5706, USA*

Accepted 23 December 2003

Abstract

Dynamic TOPMODEL is applied to the Maimai M8 catchment (3.8 ha), New Zealand using rainfall–runoff and water table information in model calibration. Different parametric representations of hillslope and valley bottom landscape units (LU's) were used to improve the spatial representation of the model structure. The continuous time series water table information is obtained from tensiometric observations from both near stream (NS) and hillslope (*P5*) locations having different responses to rainfall events. For each location, and within an area equivalent to an effective model gridscale (25 m^2), a number of tensiometer readings at different depths were available (11 for the NS site and nine for the *P5* site). Using this information a distribution of water table elevations for each time step at each location was calculated. The distribution of water table elevations was used to derive fuzzy estimates of the water table depth for the whole time series that includes the temporal variability of the uncertainty in the observations. These data were used to constrain the spatial representation of the model having previously conditioned the model using the rainfall–runoff data. Model conditioning was assessed using the Generalised Likelihood Uncertainty Estimation procedure.

Results show that many combinations of parameter values for the two LU's were able to simulate the rainfall–runoff data. Further constraining of the model responses using the fuzzy water table elevations at both locations considerably reduced the number of behavioural parameter sets. An evaluation of the distributions of behavioural parameter sets showed that improvements to the model structure for the two LU's were required, especially for simulations of the response at the hillslope location.

Keywords: Dynamic TOPMODEL; Generalised likelihood uncertainty estimation; Water table uncertainty; Parameter constraining; Fuzzy rules; Multicriteria calibration

1. Introduction

A pragmatic and realistic approach to environmental modelling should recognise that all model structures, regardless of their complexity, are to some extent in error (Beven, 1989, 2002; Grayson et al.,

* Corresponding author. Tel.: +44-1524-593563; fax: +44-1524-593985.
E-mail address: j.freer@lancaster.ac.uk (J.E. Freer).

0022-1694/$ - see front matter © 2004 Elsevier B.V. All rights reserved.
doi:10.1016/j.jhydrol.2003.12.037

1992). This can be attributed to two main factors: (1) that our perceptual model is based on imperfect knowledge, and (2) that the formulation of a model necessitates the use of highly simplified mathematical constructs that cannot represent all the details of the many interacting processes within a natural system. Furthermore increasing model complexity, or explanatory depth, increases the possibility that the amount and type of observational data at hand will be inadequate to fully assess model performance. Such data limitations would be especially apparent for semi-distributed or distributed model constructs where the individual spatial components are rarely tested locally.

Model evaluation is often made at the catchment scale using stream discharge data. The use of discharge data alone has been shown to have weaknesses in the identification of model structures and parameters (e.g. Freer et al., 1996). This understanding has led to discussions of model identifiability (Sorooshian and Gupta, 1985; Beck and Halfon, 1991) and of the equifinality of model structures and parameters (Beven, 1996; Beven and Freer, 2001b). Increasingly, recent papers have shown that being more thoughtful about the specification of objective functions or performance measures (PM's) and/or the use of multiple objectives ensures that best use is made of limited data in model calibration/evaluation (Gupta et al., 1998; Thiemann et al., 2001; Wagener et al., 2001; Seibert and McDonnell, 2002; Freer et al., 2003). One way of potentially improving the assessment of models has been to introduce multi-response data that describe different characteristics of the system. These measures may improve the identification of model structures and associated parameters without increasing the complexity of the model (Troch et al., 1993). There have now been a number of studies where this has been explored (Kuczera, 1983; de Grosbois et al., 1988; Bloschl et al., 1992; Grayson et al., 1992; Koide and Wheater, 1992; Lamb et al., 1997; Mroczkowski et al., 1997; Franks et al., 1998; Kuczera and Mroczkowski, 1998; Guntner et al., 1999; Motovilov et al., 1999; Vertessy and Elsenbeer, 1999; Anderton et al., 2002a; Aronica et al., 2002; Blazkova et al., 2002; Uhlenbrook and Leibundgut, 2002).

The introduction of data other than discharge into the calibration process has not always produced satisfactory results. Stephenson and Freeze (1974) and Koide and Wheater (1992), in similar studies using detailed 2D distributed hillslope models calibrated from comprehensively sampled tensiometer and piezometer data, both noted difficulties in the calibration of their models due to numerous data and model simplification/initialisation factors. Grayson et al. (1992) found that the 'measurement of catchment response in sufficient detail' (i.e. limitations imposed by data sparseness) was a limiting factor in the spatial validation of the THALES model. Hooper et al. (1988) found that using a combination of rainfall–runoff and geochemical data to identify a model with only six parameters called into question 'the structural validity of more highly parameterised rainfall–runoff models used in water quality prediction'. More recently Anderton et al. (2002b) found difficulties in using limited soil moisture and phreatic surface information in the validation of the SHE-TRAN model due to both the sparseness of the data and the 'mismatch' of the measurement scale to the model gridscale (see detailed discussions on using/interpreting spatial patterns for hydrological modelling in Grayson and Bloschl, 2000).

While the introduction of new data sources (beyond that of discharge) into the assessment of models can increase model identifiability, a number of issues may bias the conclusions:

- The data are uncertain (Sherlock et al., 2000). That is, for many data types there may be an inevitable degradation of quality and/or of the ability of the data to be representative of the system of interest.
- The data may not be appropriate. That is, the phenomenon being represented by the data may not be commensurate with the model formulation, therefore direct comparisons through the specification of simple objective functions may not be realistic
- The observations may be at the wrong scale. That is, observations may be at a different scale to the model scale. For scale discrepancies there might be a range of observed behaviour that is both large and inconsistent over time periods for the effective model gridscale.

As a result of these points, different performance measures may be required to match model assessment

with the appropriate level of data quality, representativeness and scale. The error associated with models and data and the limitations of current data technologies directs the practitioner towards an assessment of models that is inherently probabilistic (see for example the use of uncertain saturated area observations in Franks et al., 1998). A probabilistic assessment allows for multiple parameterisations and/or model structures. Nevertheless, rejection is often difficult because of the limitations in the available data or because of our 'imperfect knowledge' of the system under study.

A number of calibration methodologies for this type of approach have been developed, each having to a greater or lesser extent assumptions regarding the nature of the error structure, the sources of error and the complexities of the multidimensional parameter space response surface. This paper introduces multi-response data (discharge and tensiometric information) into the assessment of a hydrological model (Dynamic TOPMODEL) within the uncertainty analysis framework Generalised likelihood uncertainty estimation (GLUE). Both stream discharge and multiple tensiometric readings are used for two topographically distinct sites within the Maimai catchment, New Zealand. The variability in the multiple readings at each site are characterised as a time-variable fuzzy objective function in a way that is more appropriate to the effective model gridscale and the uncertainty within multiple observations. To reflect the differences in these two topographically different sites Dynamic TOPMODEL is configured for two Landscape units (LU's) one being a Hillslope (HS_{LU}) and the other a Valley Bottom (VB_{LU}), each having independently sampled parameter values. The parameter interactions between the two LU's are assessed and conclusions are drawn as to the usefulness of uncertain (fuzzy) gridscale information in constraining model parameters. Specifically, we address the following questions within the context of this general aim of simulating the discharge and water table (∇_{wt}) responses:

- Can we meet discharge and/or tensiometer criteria for more than one source of information?
- How can fuzzy rules be applied to imperfect and imprecise knowledge when the error structures are time variant?
- How can we constrain model responses and the efficiency of sampling?
- How can we improve the Dynamic TOPMODEL structure and parameter representation?

This paper builds upon a recent paper by Seibert and McDonnell (2002) that explored soft data measures (i.e. very fuzzy notions of how the experimentalist views the catchment rainfall–runoff process) by examining specific internal data sets common to many experimental catchments around the world.

2. The study site

The Maimai M8 catchment is located in the Tawhai State Forest, North Westland, South Island, New Zealand. It is one of eight small adjoining catchments that have been studied since 1974 as part of a land use change study. The layout of the catchment is shown in Fig. 1a–d.

Mean annual gross rainfall in this area is approx. 2600 mm, producing some 1550 mm of runoff from 1950 mm of net rainfall (Rowe, 1979), with little seasonal variation. The Maimai catchments are highly responsive to rainfall, Pearce and McKercher (1979) reported that quickflow represents 65% of annual runoff (39% of total rainfall), as defined by Hewlett and Hibbert (1967) separation method. Sklash (1990) commented that 'The Maimai catchments are among the most hydrologically responsive forested headwater catchments documented'

The surficial geology of Maimai catchment is firmly compacted, moderately weathered, early Pleistocene conglomerate, which is known as the Old Man Gravels and has been described as 'effectively impermeable' by Mosley (1979). The relief of the catchment is in the order of 100–150 m, with steep (average 34°), short (less than 30 m) slopes (see Fig. 1a). Soil development has weathered the conglomerate to form (as a broad classification), Blackball Hill soils (Mew et al., 1975). These soils are spatially quite variable in both depth (0.2–1.8 m) and character, having a thick well developed upper humic horizon (mean 170 mm, Webster (1977)). The upper mineral soil has been found to have an average saturated hydraulic conductivity of 250 mm h^{-1}

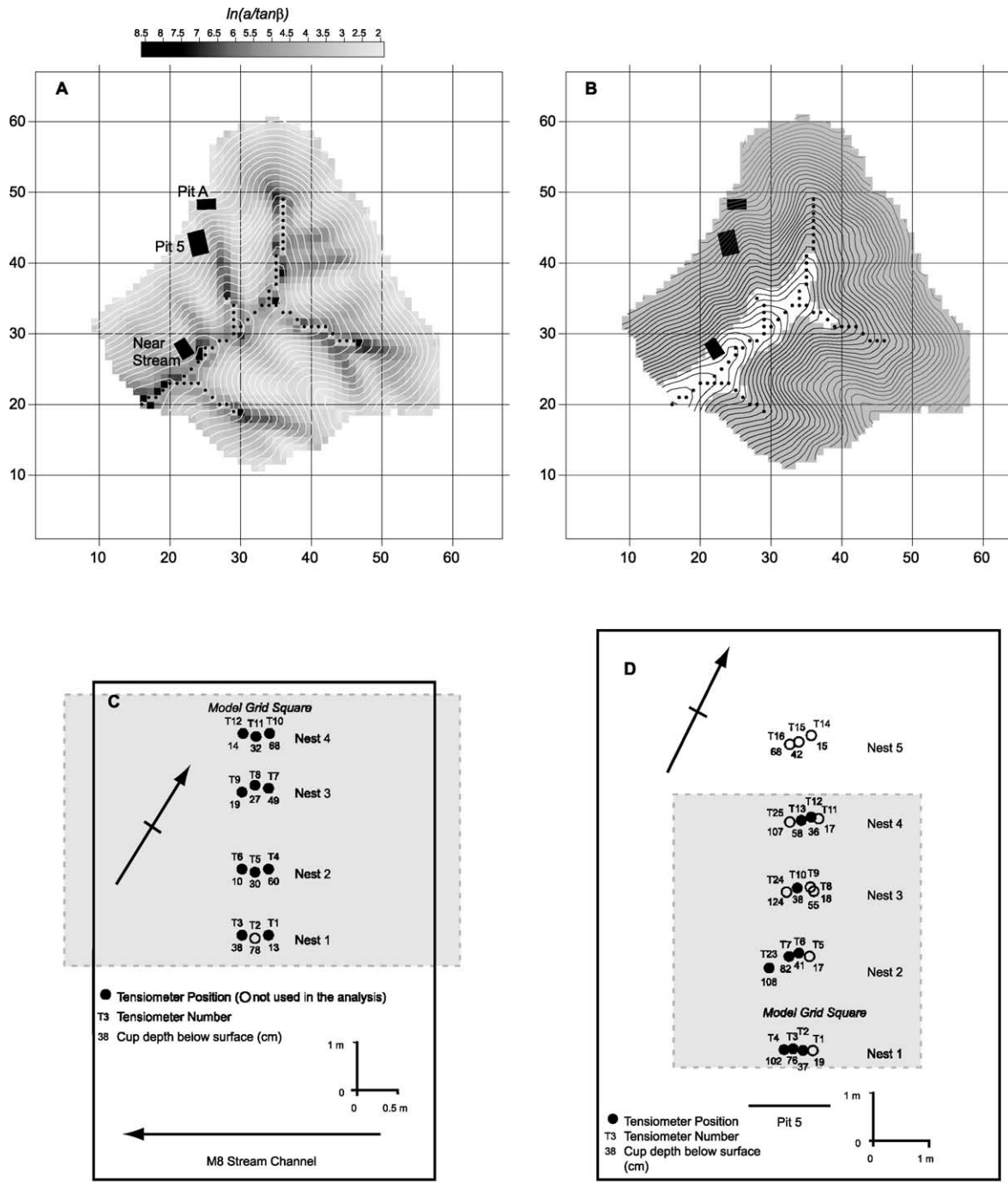

Fig. 1. Maimai M8 catchment: (a) The spatial variability of the ln (a/tanβ) index and (b) the spatial distribution of the VB_{LU} and HS_{LU} LU's. Details of the study area showing the position of the tensiometer instrumentation at (c) the Near Stream and (d) the Pit 5 sites.

(Webster, 1977). However, using a Guelph permeameter, McDonnell (1989) found this value to be highly variable, ranging from <5 mm h^{-1} in poorly drained hollows to the value reported by *Webster* in well drained nose slopes. The average infiltration capacity of the soil surface has been reported by Webster (1977) as 6100 mm h^{-1}.

The vegetation of the catchment is classified as a mixed evergreen forest, the main cover being dominated by southern beech, podocarps and broadleaf hardwoods. The forest is multi-storied, the understorey consists of dense tree fern and shrubs and has a ground cover of ferns and herbs (Pearce et al. 1986). A more detailed physical description of the Maimai M8 catchment can be found in Rowe et al., (1994); McGlynn et al. (2002).

2.1. The tensiometer study sites

The layout of the Maimai M8 catchment is shown in Fig. 1, and has been extensively documented by Pearce et al. (1986). The intensive monitoring of the 0.3 ha subcatchment and the Near Stream (NS) site was undertaken over a number of storm events during September to December 1987 (McDonnell, 1990). The data collected included tensiometer, trough flow, and chemical and isotopic tracer samples, as well as hydrometric data based on a 10 min time step. Two tensiometer sites were used from this intensive study, these being the NS (Fig. 1c) and *P5* (*P5*—Fig. 1d) sites, both of which have been reported in McDonnell (1990) with regard to 3D matric and total potential (ϕ) responses. Tensiometers were situated away from any visible cracks and voids to ensure they characterised only the changes in the soil matrix (McDonnell, 1990). The topographic position of the two sites differs considerably (see Fig. 1a), with the NS site having a close proximity to the stream channel (<4 m) and the *P5* site on a steeper upslope section (some 40 m from the stream channel). Consequently the data provide a good test of the possible variation in water table responses in two topographically distinct areas of the catchment. These two catchment positions have been shown to differ considerably in their groundwater response (McDonnell, 1990), soil water isotopic composition (McDonnell et al., 1991) and solute concentrations (McGlynn and McDonnell, 2003). The variations in soil properties between these two sites are given in Table 1 and will be referred to in later sections.

The *P5* site consisted of an electronically multiplexed and logged array of 32 tensiometers (arranged within a grid 6 m by 1 m), whereas the NS site had 24 tensiometers (in 4 m by 0.5 m) that were linked via a fluid scanning switch to a single pressure transducer. The *P5* site had continuous logged data, which were recorded at the same time for all tensiometers. Due to the fluid scanning switch at the NS site, a single reading was taken in rotation at a maximum resolution of one minute increments, although this increment sometimes increased to 5 min for short (recession) periods. Details of the tensiometer design and performance are given in McDonnell (1993). The tensiometers ranged in their depth below the soil surface from 15–124 cms for the *P5* site and 10–78 cms for the NS site.

Readings from the two sites were not available for the complete discharge period (see Fig. 2). The data

Table 1
Local DTA values, soil and topographic characteristics for both the Near Stream and Pit 5 sites as well as average data for the Maimai Catchment

Site	DTA results			Observed field data		
	ln (a/tanβ)	Acc. Area	Soil depth (m)	Slope (°)	Total porosity (%)	Saturated conductivity (m/h)
Near stream[a]	4.03	183.0	0.5	15	52	–
Pit 5[a]	3.04	101.9	1.5	34	68	–
Catchment[b]	–	–	0.6	–	45[c]	0.01–0.3[d]

[a] Observed field data from McDonnell, J.J. (pers comm.)
[b] Data taken from McGlynn et al., 2002.
[c] Top 0.17 m organic horizon 86% total porosity (39% macroporosity).
[d] Soil Infiltration rate 6.1 m/h.

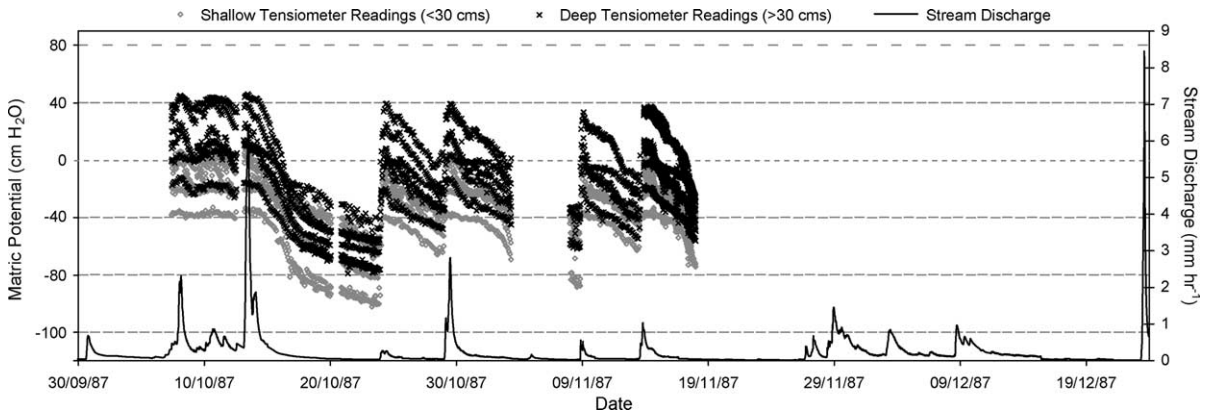

Fig. 2. Near Stream site shallow and deep tensiometer readings adjusted to matric potentials. All available tensiometer responses are plotted against catchment discharge for the whole of the observation record used in this study.

collected for the *P5* site were available from 2/10 at 19:40 to 17/12 at 14:30, and for the NS site from 7/10 09:20 to 18/11 at 00:00. Within these limits the data had a considerable number of short and long 'breaks' (equipment failure etc.). Most of the longer breaks occurred during recession periods, however, some of the smaller disruptions occurred during events, or meant that some of the smaller storm events were not available.

McDonnell (1990) detailed results from the NS site for tensiometers T1–9 and from the *P*5 site for tensiometers T1–16 and T23–25 for the October 29th storm event. There were considerable difficulties in creating a coherent data set for an extended period, mainly due to periods of failed tensiometers. The intention was to incorporate as many tensiometer readings as possible into the calculation of a ∇_{wt} series, so that a proper account was taken of the variability of the tensiometer response at a scale that was consistent with the model gridscale (see discussion by Bathurst and O'Connell, 1992). Due to problems of equipment failure and extreme electrical noise, not all of the tensiometers at the two sites were used. Furthermore, shallow tensiometers at the *P5* site were sensitive to the wetting front propagation down through the soil profile during precipitation events, these sensitivities would not be directly related to the ∇_{wt} formation from the soil-bedrock interface and were also excluded. This resulted in nine tensiometers at the *P5* site and 11 at the NS site that could be used in the following methods. These tensiometers covered areas of 4.5 m × 1 m and 4 m × 0.5 m, respectively, and are shown as filled circles in Fig. 1c and d along with their cup depth below the soil surface. Notwithstanding, the tensiometer responses are consistent with similar responses on steep wet hillslopes published more recently on comparable slopes in Oregon (Torres et al., 1998), Japan (Uchida et al., 2001) and Singapore (Rezaur et al., 2002).

3. Methods

3.1. Calculation of water table responses at both tensiometer sites

Tensiometer readings have positive matric potential when the porous cup is below the water table surface, negative matric potential when the tensiometer cup is above the water table surface and zero values at the water table surface. Variations of matric potential at the NS site for all tensiometer readings used in this study are shown in Fig. 2 for the whole of the study period. Fig. 2 shows that positive (+ve) matric potentials are observed for much of the study period. For the *P5* site +ve potentials were more transient, having steeper recessions (which are reflected in the ∇_{wt} variations shown for both sites in Fig. 6).

The relationships between −ve matric potentials and soil water content can be complex and have been well documented (Kosugi and Inoue, 2002; Torres and Alexander, 2002). Soil water retention curves have been determined for many different soil types

and generally show hysteresis behaviour between the wetting and drying curves. Burt and Butcher (1985; 1986) developed a simple methodology that used average gradient of soil water potentials (from a number of tensiometers at different depths) to predict the depth of the ∇_{wt} at the soil-bedrock interface. Using field calibrations obtained from Butcher (1985)] they suggested that the average gradient (at their experimental site at Slapton Wood, UK) under − ve tensions was 1.2 cm soil water potential per cm soil depth (a linear relationship). We used the Butcher, 1985 method to develop a relationship between − ve soil water tensions and apparent depth to the ∇_{wt} at Maimai. The ∇_{wt} is directly inferred during periods where the deepest tensiometer is below the ∇_{wt} surface (in + ve tension). Matric potentials, expressed in terms of head units (m), were linearly adjusted to a ∇_{wt} surface, for both + ve and − ve readings, by correcting readings to the ground surface datum by;

$$Z_{wt}(t) = Z_T(t) - \phi_T(t) \quad (1)$$

where Z_T is the depth of the tensiometer (m) and ϕ_T is the matric potential reading of the tensiometer [m H_20] at time t. It should be noted that Eq. (1) is only valid if it is assumed that vertical soil water fluxes are negligible, suggesting that the soil is in equilibrium and total potentials are constant throughout the soil profile. Fig. 3a and b show for the recession period of the October 29th storm event the relationship between − ve matric potentials and height above the water table for all tensiometers at the NS (Nest 4) and *P5* (Nest 1) sites (see Fig. 1) during periods where the deepest tensiometer is in + ve tension (i.e. T10 and T4, respectively). A recession period is chosen to avoid wetting fronts affecting tensiometer readings during precipitation events. Significantly fewer points were available for the *P5* site because the peak response was much more transient so that + ve tensions were not maintained at T4. For the NS site a linear relationship provides a good correlation between − ve tension and height above ∇_{wt}($R^2 = 0.94$), having a similar slope gradient to that found by Butcher (1985), namely 1.16 cm soil water potential per cm soil depth. For the *P5* site the linear relationship does not seem to hold as well ($R^2 = 0.91$), the slope gradient is much higher (2.4 cms/cm) and the relationship for the site appears to be only quasi-linear having a lower gradient for smaller − ve tensions. For these hillslope soils a more appropriate relationship is found using a second order polynomial ($a = 1.192, b = 0.048, R^2 = 0.97$). Such non-linearity may be the result of the − ve matric potential gradients being non-uniform in the unsaturated zone for these soil types (note that the initial slope gradient is again similar to the results of Butcher (1985)). Confidence in this relationship increased further after calculating the predicted ∇_{wt} depth for all tensiometers at *P5* (Nest 1) over a much longer recession period (i.e. for a higher − ve potential range) the results of which are shown in Fig. 3c. The variability in the ∇_{wt} predictions over the recession period is low but tends to increase with increasing ∇_{wt} depth (to a maximum in this case of 20 cm). However, such variability within local tensiometer nests is much less than the ∇_{wt} predictions between the local tensiometers nests (i.e. the variability at the effective model gridscale) for both the NS and *P5* sites (see below and Section 3.2), including periods where + ve tensions were observed at multiple sites.

The methods described above allowed + ve tension (using Eq. (1)) and − ve tension readings using the linear and polynomial relationships for the NS and *P5* sites, respectively, to be used to predict the ∇_{wt} variations for the whole study period. To summarise the variability of ∇_{wt} predictions throughout the study period Fig. 4 shows the variability in the range of ∇_{wt} observations for different depths (classified by the observed mean depth for each timestep), for the minimum to maximum and 25th to 75th inter-quartile range for both the NS and *P5* sites. Fig. 4 also gives the percentage of time that each depth occurred during the series, this clearly showing the more transient nature of shallow ∇_{wt} observations at the *P5* site with higher frequencies of occurrence being skewed towards deeper ∇_{wt} depths. These plots show that the mean and inter-quartile ranges of ∇_{wt} observations vary with depth, increasing with increasing depth for the NS responses and with depths associated with more rapidly changing ∇_{wt} fluctuations during events for the *P5* site (see Fig. 6).

3.2. A fuzzy measure of water table responses at the model gridscale

We have identified that the tensiometer responses used in this study are not themselves wholly accurate

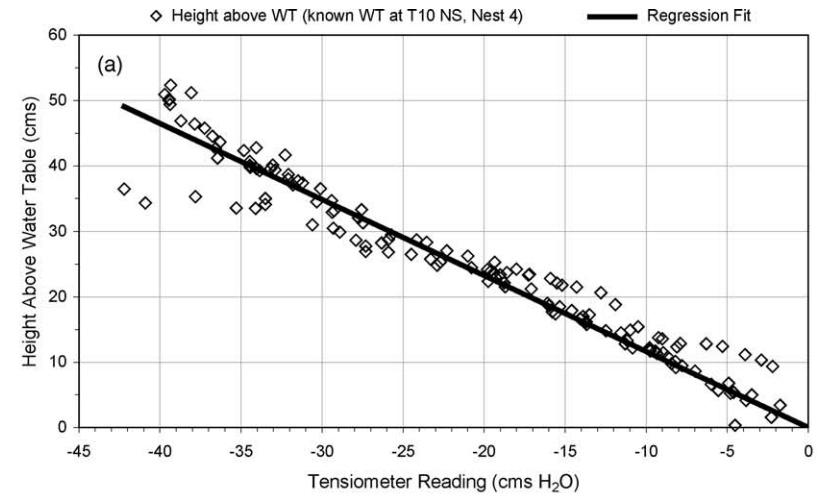
Height above WT (known WT at T10 NS, Nest 4)
Regression Fit
(a)
Height Above Water Table (cms)
Tensiometer Reading (cms H2O)

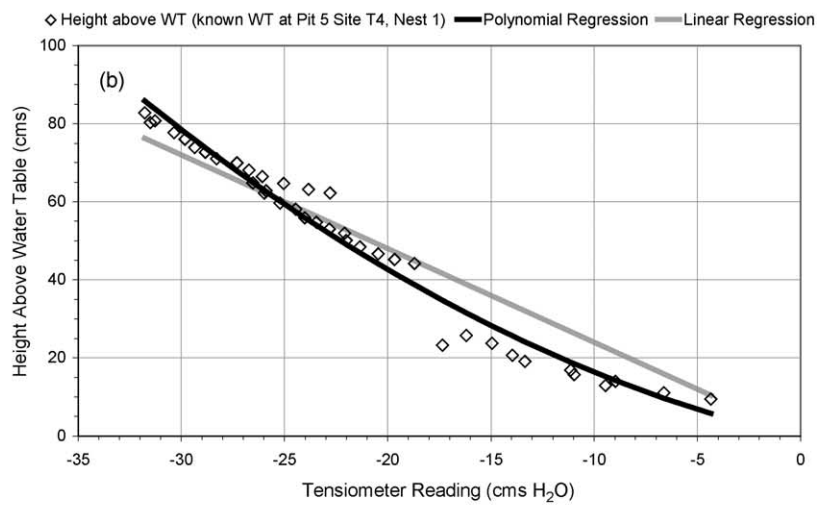
Height above WT (known WT at Pit 5 Site T4, Nest 1)
Polynomial Regression
Linear Regression
(b)
Height Above Water Table (cms)
Tensiometer Reading (cms H2O)

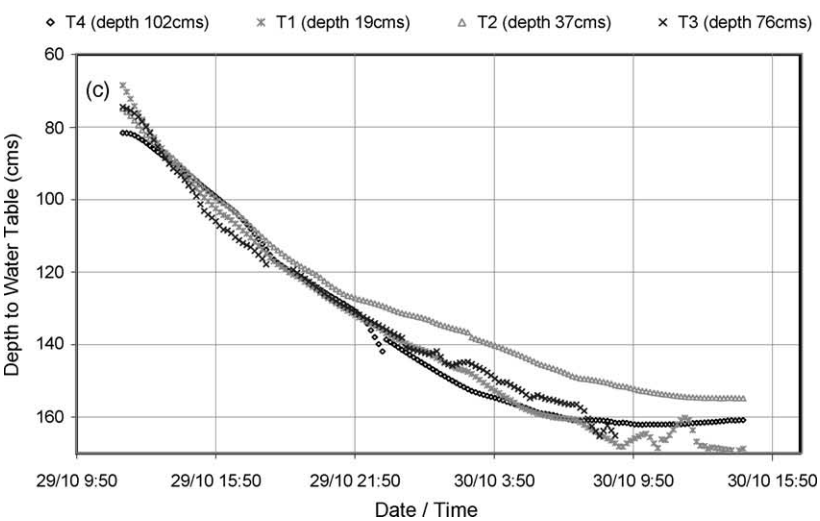
T4 (depth 102cms)
T1 (depth 19cms)
T2 (depth 37cms)
T3 (depth 76cms)
(c)
Depth to Water Table (cms)
29/10 9:50
29/10 15:50
29/10 21:50
30/10 3:50
30/10 9:50
30/10 15:50
Date / Time

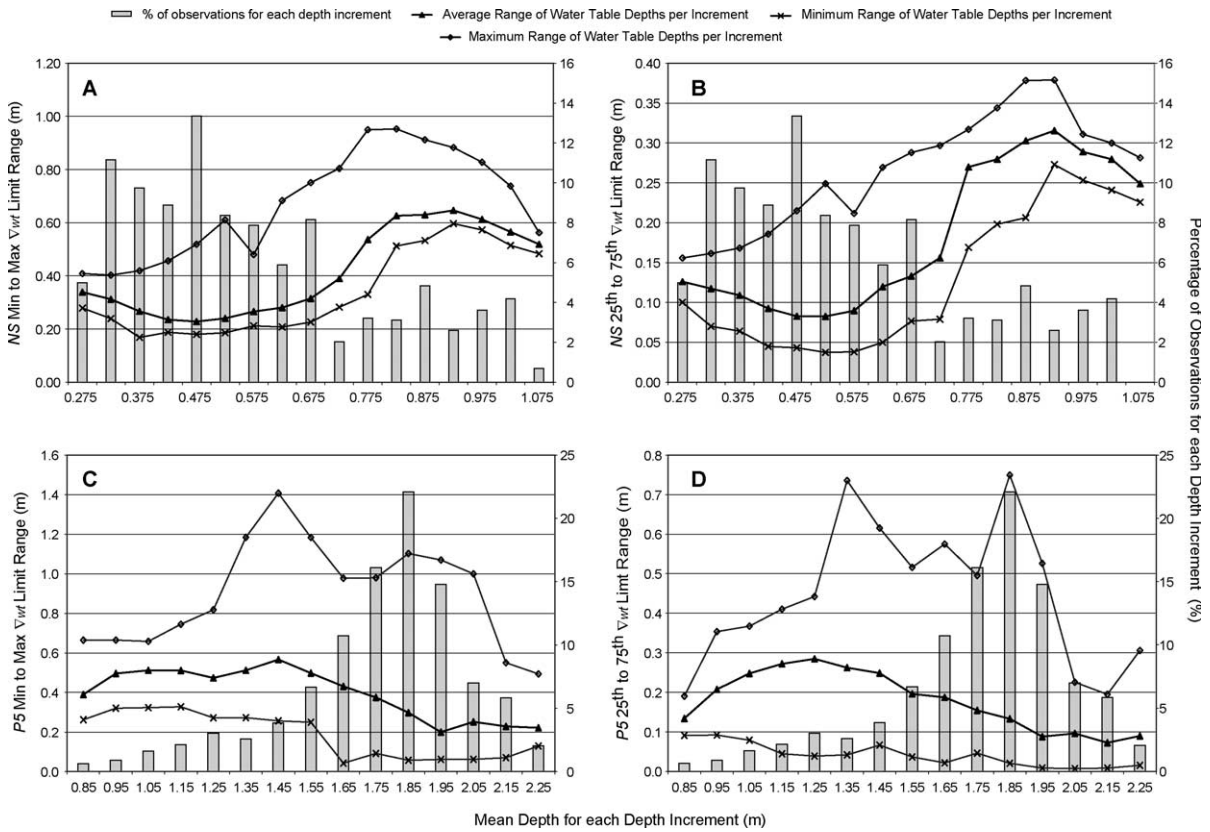

Fig. 4. The variability in the range of ∇_{wt} levels for the two distribution limits used to define the fuzzy numbers for each timestep (i.e. the min–max for the *support* and the 25th and 75th for the *core* values of the fuzzy number) summarised for the whole of the observed data series by categorising the readings at each time step by the mean ∇_{wt} level. The range and mean ∇_{wt} levels are determined separately for each tensiometer site from the variability in all tensiometer observations adjusted to depth using the regression relationships shown in Fig. 3. Results for the Near Stream site are shown for the *support* limits in (A) and the *core* limits in (B), with the same limits shown for the Pit 5 site in (C) and (D) respectfully. For all plots the frequency that each mean ∇_{wt} category is sampled (i.e. the number of time steps) for the whole data series is also shown.

predictions of the ∇_{wt} as seen in the regression relationships presented in Fig. 3. Furthermore significant local variations of the ∇_{wt} are observed at a scale that is more commensurate with the model gridscale and the magnitude and distribution of these variations change with time. What we require therefore is a performance measure that for each timestep and at the model gridscale reflects the noise in the data, the variability in the timings of the ∇_{wt}, and the uncertainty in the information expressed within the regression relationships between $-$ve tensions and height above the ∇_{wt} surface. Taking into account the standard errors in the regression relationships would lead to a wider range of uncertainty in the ∇_{wt},

Fig. 3. The relationships between observed $-$ve matric potentials and heights above a known ∇_{wt} (at least one tensiometer in $+$ve tension) for (A) the Near Stream site, Nest 4 and (B) the Pit 5 site, Nest 1. The plots show the regression curves used to describe these relationships for both cases. For the Pit 5 site, Nest 1 (C) shows for each tensiometer the depth to the water table for an extended recession period calculated using the regression relationship shown in (B).

but given the high correlations found in these relationships (see below) the resulting increase in uncertainty would be small relative to the range of predictions between tensiometer readings. Therefore so as not to unduly bias the assessment of model performance a fuzzy additive definition of the performance measure was used, having the following form of membership function (see Ross, 1995):

$$L[M(\Theta_i|Y_T,W_T)] = \sum_{t=1}^{n} \begin{cases} 0 & z_t \geq {}_{\max} w_t \\ \dfrac{z_t - {}_{75} w_t}{{}_{\max} w_t - {}_{75} w_t} & {}_{75} w_t \leq z_t \leq {}_{\max} w_t \\ 1 \quad \ldots\text{if}\ldots & {}_{25} w_t \leq z_t \leq {}_{75} w_t \\ \dfrac{z_t - {}_{\min} w_t}{{}_{25} w_t - {}_{\min} w_t} & {}_{\min} w_t \leq z_t \leq {}_{25} w_t \\ 0 & z_t \leq {}_{\min} w_t \end{cases} \quad (2)$$

where $M(\Theta_i|Y_T,W_T)$ indicates the ith model simulation run, conditioned on input data Y_T and observations W_T. For each timestep t the simulated local ∇_{wt} depth z_t is compared to the distribution of ∇_{wt} observations defined by the *core* (the 25th ($_{25}w_t$) and 75th ($_{75}w_t$) quartiles) and the *support* (the min ($_{\min}w_t$) and max ($_{\max}w_t$) values) of the fuzzy membership function. Essentially Eq. (2) defines a trapezoidal fuzzy membership set (see Fig. 5) for the observed ∇_{wt} responses, the characteristics of which depend on the distribution of the local ∇_{wt} depth at each timestep. The *core* of the set being the range of depths where we believe that the simulated z_t would be a complete and full member of the observations and the *support* being the range of depths either side of the *core* where we have a nonzero membership (i.e. that we become less sure that the simulation is a member the closer this value approaches the *support* limits).

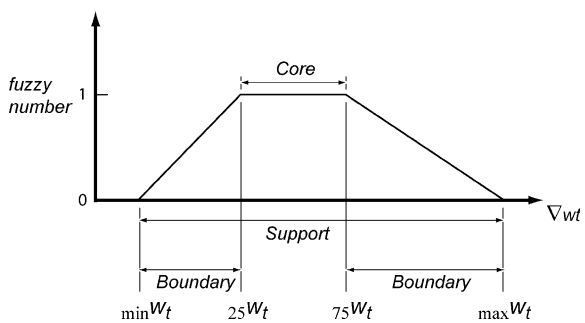

Fig. 5. An example of the construction and terminology of a fuzzy number used in this study. The limits ($_{\min}w_t$, $_{25}w_t$, $_{75}w_t$ and $_{\max}w_t$) are determined using Eq. (2).

The assignment process that defines the form of the membership function can involve many methods, ranging from intuition (i.e. what is the range of saturated area in this catchment that we believe is possible?) to the use of more formal methods such as inductive reasoning and the use of fuzzy statistics (see Ross, 1995). Membership functions may or may not have a core range and or have much more complex forms (e.g. multi modal, subnormal and non-convex) depending on the observations that are available. The assignment procedure used here would formally be known as an inference procedure (i.e. deductive reasoning from some knowledge of the system). In this case using the 5th and 95th percentiles as the support limits rather than the minimum and maximum values was rejected as there was felt to be no justification for totally rejecting the possibility that the outer ∇_{wt} readings were correct. The trapezoidal measure was chosen as this represented a compromise between the difficulties of defining what was the 'best' ∇_{wt} observation at each timestep (a membership function without a core range) and the advantage of favouring mid-range ∇_{wt} values that would not be the case using a crisp set (i.e one without *boundaries*—see Fig. 5). Fig. 6 shows the resultant support limits for the ∇_{wt} membership function (the core is not shown for clarity) and the individual ∇_{wt} observations at both tensiometer sites for all timesteps where data are available. These results clearly show that the amount of uncertainty in the ∇_{wt} surface varies considerably during the study period, that this variation is significant for similar ∇_{wt} depths at different time periods (especially for *P5*) and that each tensiometer study site has different characteristics of variability.

3.3. The hydrological model—dynamic TOPMODEL

The new Dynamic TOPMODEL version is briefly described below to allow the reader to understand the spatial context of the model structure and associated parameters applied to Maimai catchment. For a more detailed treatment of the model application and model theory the reader is referred to the paper by Peters et al.

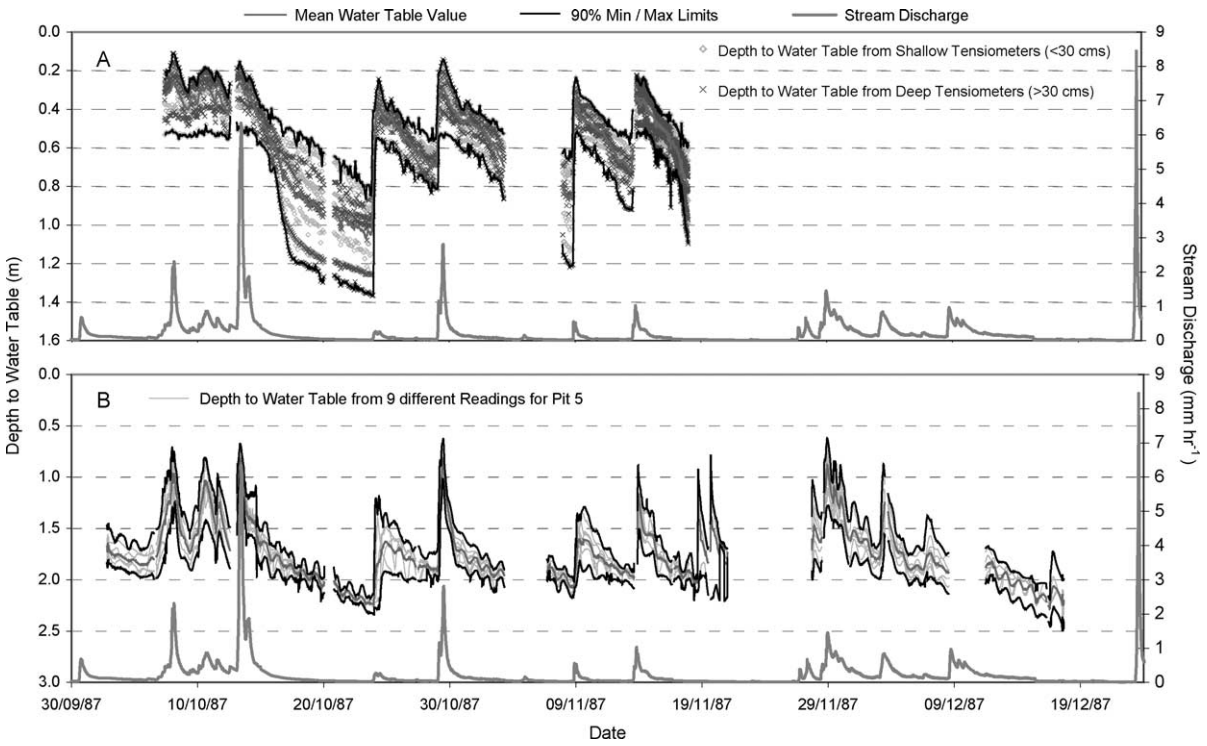

Fig. 6. Observed water table responses calculated from the tensiometer data for both (A) Near Stream and (B) Pit 5 tensiometer sites. The plot shows the resultant upper and lower min and max limits for the water table responses defining the model gridscale variability of the observations.

(2003) and to the original paper on Dynamic TOPMODEL by Beven and Freer (2001a).

Dynamic TOPMODEL (Beven and Freer, 2001a) is a new version of TOPMODEL that relaxes some of the assumptions of the original form (Beven and Kirkby, 1979) following critiques of TOPMODEL by Barling et al. (1994); Beven (1997), and Wigmosta and Lettenmaier (1999). This new formulation allows for local accounting of hydrological fluxes and storages, relaxing the quasi steady state assumption of a water table parallel to the local surface slope expressed through the derivation of the ln (a/tan β) index of Kirkby (1975). Therefore the dynamics of the subsurface saturated zone during wetting and drying event periods (expanding and contracting) can be simulated. Previous field evidence had suggested that the original assumption of an effective upslope contributing area extending to the catchment divide during wetting-up periods was thought to be unrealistic (Barling et al., 1994; Guntner et al., 1999). Beven (1997) suggested that the overestimation of the accumulated upslope area 'a' was being compensated in the results by generally high transmissivity values, this being seen in original TOPMODEL applications. Dynamically varying upslope contributing areas 'a' are conceptualized in a simple form with the addition of the parameter S_{max} (the maximum effective deficit of subsurface saturated zone), which in a simple form, as in this example, restricts down slope flow only to areas where the local deficit $s_i \geq S_{max}$ Areas with shallow regolith depths (small S_{max}) and areas near the catchment divide, would be more likely to 'disconnect' upslope areas during recession periods. Beven and Freer (2001a) found the best behavioural simulations of discharge at Slapton Wood catchment in the UK occurred with a dynamically varying upslope contributing area (i.e. when S_{max} became active). However, good/acceptable (behavioural) simulations were also obtained for simulations where no change in the upslope contributing areas was predicted.

Without any further information on the spatial variability of hydrological processes a 2D classifier matrix $[a, T_0 \tan \beta]$ is used as measure of hydrological similarity, where T_0 is the transmissivity measured in the direction of downslope flow, $\tan \beta$ the local slope angle, and a as before. Using a 2D classification matrix that includes 'a' ensures the resulting hydrologically similar units (HSU's—now used as the local hydrological accounting units), maintain a general continuity of flow in a downslope direction but whose fluxes are dynamically variable. Topographic analysis allows the calculation of a transition probability matrix for a water drop to move from one class to another (an extension of the multi-flow algorithms of Quinn et al. (1991)). In this way, the water balance for each HSU can be solved. Transfers between HSUs are calculated using a kinematic wave approximation, where both the upslope (for inputs) and local (for outputs) storages are required. Flux volumes are a function of the storages and the $T_0 \tan \beta$ values in each case (Beven and Freer, 2001a). As with the original TOPMODEL, an exponential transmissivity profile and a constant effective storage coefficient are assumed in each LU. Experience in a number of catchments in different countries suggests that the transition from hillslope to valley bottom LU's is often quite marked and will require the use of different parameter values in each LU.

The model also allows for the spatial organisation and connectivity of different HSU's, each having potentially different functional forms of hydrological (and/or other) responses. Including different functional forms requires some knowledge of the spatial variability of hydrological response, which may often be limited (especially within the subsurface) at a scale pertinent to catchment scale responses. Peters et al. (2001) conceptualised Dynamic TOPMODEL for Panola Mountain Research Watershed (PMRW) to include the spatial variability of distinct LU's, primarily though the distribution of regolith depths. These LU's were assumed to have different hydrological/physical characteristics that were controlling hydrological response and therefore required the definition of different parameter ranges and/or model structure. In this study the catchment has been separated into two LU's, a HS_{LU} and a VB_{LU} component (see Fig. 1), the general break in slope between the VB_{LU} and HS_{LU} areas defined the spatial extent of these units. Two LU's were identified primarily to study the interactions between parameter sets when simulating the discharge and the NS and *P5* ∇_{wt} responses. The spatial variability of hydrological response due to additional topographic features at Maimai (i.e. ridges and hollows), is characterised explicitly in the model using the classifer matrix of hydrological similarity (described above).

A previous application at Maimai using the original form of TOPMODEL by Freer (1998) showed that no parameter sets (using homogeneous parameter values) could be identified that satisfactorily simulated the ∇_{wt} responses at both sites, although when treated individually behavioural parameter sets could be identified for each site. The functional differences in the LU's are here expressed by the differences in the parameter ranges for each unit (see Table 2), i.e., the same functional *form* is retained for each LU, including the assumption of an exponential decline in transmissivity with depth.

Table 2
Parameter descriptions and ranges for the VB_{LU} and (in {}'s) the HS_{LU} for the Monte-Carlo simulations for run_1

Parameter	Units	Lower limits[a]	Upper limits[a]	Description
SZM	[m]	0.001 {*0.005*}	0.012 {*0.017*}	Form of the exponential decline in saturated hydraulic conductivity with depth
$\ln(T_0)$	[$m^2\ h^{-1}$]	−7.0 {−7.0}	3.0 {3.0}	Effective lateral saturated transmissivity
SR_{max}	[m]	0.005 {0.005}	0.08 {0.08}	Maximum soil root zone deficit
SR_{ini}	[m]	0.00 {0.00}	0.01 {0.01}	Initial root zone deficit
CHV	[$m\ h^{-1}$]	250 {250}	1500 {1500}	Channel routing velocity
T_d	[h]	0.10 {0.10}	40.0 {40.0}	Unsaturated zone time delay
$\Delta\theta$		0.05 {0.01}	0.60 {0.30}	Effective porosity
S_{max}	[m]	0.60 {0.60}	2.00 {2.00}	Maximum effective deficit of the subsurface storage zone

[a] Parameter upper and lower ranges for both the valley bottom and hillslope.

The 2-LU model has 14 parameters (*CHV* and SR_{init} are sampled once for each simulation, then assumed constant for all LU's). The catchment was divided using digital terrain analyses (5 m^2 DEM) into 41 HSUs for the model simulations.

3.4. GLUE simulations of discharge and water table information

Freer (1998) used the original form of TOPMODEL applied to Maimai for both discharge and ∇_{wt} simulations (at the NS and *P5* sites) as reported here but using a weighted Nash efficiency measure (weights calculated from the uncertainty in the ∇_{wt} depth) within the GLUE procedure. As noted above no homogeneous catchment parameter sets could be found that simulated the ∇_{wt} responses at both tensiometer sites. Recently Beven and Freer (2001b), also using the original form of TOPMODEL, analysed multiple years of discharge data at Maimai and found that once uniform prior distributions had been constrained using 1 year of data, subsequent years did little to constrain parameter estimates further. This paper extends these analyses by assessing multi-objective variations in model performance for dynamic TOPMODEL within the GLUE methodology using fuzzy performance measures. The multi-objective data in this case are the discharge and the ∇_{wt} information at both tensiometer sites. For the initial simulation runs all parameters listed in Table 2 were randomly assigned a value appropriate to the ranges specified for each LU (where appropriate). For initial simulations a uniform sampling strategy of the parameter ranges was deployed to express the lack of knowledge of the expected distribution and covariance of the parameter values. The model streamflow and ∇_{wt} predictions for the study period were compared to the observed data using one of the three Performance Measures and rejection criteria defined in Table 3. For each tensiometer site the midpoint position of the tensiometer nests was used to georeference this data with the DTM coverage. The time series of the simulated ∇_{wt} predictions for both corresponding HSU increments and the catchment outfall discharge predictions were retained for post analysis along with the parameter values for the model run. Differences among behavioural parameter sets were evaluated for each performance measure.

The GLUE simulations were conducted on a parallel LINUX PC system at Lancaster University. The system consists of 47 nodes having a combination of AMD 800, 1500 and 2600 MHz processors. The topology used was a simple master slave combination via 100 Mbps Ethernet using basic batch processing scripts for job submissions (one job per slave unit). The initial 5,600,000 simulations took 2 days to complete (on 6 fast nodes) for the 1987 study period.

4. Results and discussion

In total 6.8 million runs of the model were generated. The initial 5.6 million runs described above are referred to hereafter as run_1. To see how much the efficiency of sampling could be improved from run_1 a further 1.2 million more runs of the model (run_2) with reduced parameter ranges were generated (where these could be determined from behavioural simulations that resulted in constrained parameter ranges from run_1, see Table 4). This run also employed a uniform sampling strategy. The results presented in the following result sections are initially from run_1, but the final dotty plots and confidence limits presented in Figs. 8–10 are calculated from

Table 3
Discharge and ∇_{wt} performance measures and their acceptability criteria evaluated for the dynamic TOPMODEL GLUE simulations

Performance measure	Equation	Acceptability criteria
R^2 discharge	$L[M(\Theta_i \mid Y_T, W_T)] = (1 - \sigma_\varepsilon^2/\sigma_o^2)^{N a}$	0.6
Near stream FUZZY additive	Eq. (2) (in text)	1000 (maximum possible 2464)
P5 Fuzzy additive	Eq. (2) (in text)	2000 (maximum possible 4149)

[a] Where σ_ε^2 is the error variance; σ_o^2 is the variance of the observations and $N = 1$.

Table 4
Parameter ranges for the VB_{LU} and (in { }'s) the HS_{LU} for the Monte-Carlo simulations for run_2

Parameter	Units	Lower limits[a]	Upper limits[a]
SZM	[m]	0.003 {*0.005*}	0.012 {*0.015*}
$\ln(T_0)$	[m^2 h^{-1}]	−5.0 {−2.0}	4.0 {5.0}
SR_{max}	[m]	0.005 {0.005}	0.08 {0.08}
SR_{ini}	[m]	0.00 {0.00}	0.01 {0.01}
CHV	[m h^{-1}]	250 {250}	1500 {1500}
T_d	[h]	0.10 {0.10}	40.0 {40.0}
$\Delta\theta$		0.01 {0.01}	0.40 {0.10}
S_{max}	[m]	0.60 {0.60}	2.00 {2.00}

[a] Parameter upper and lower ranges for both the valley bottom and hillslope.

run_2, having a total number of behavioural parameters sets shown in the second part of Table 5.

4.1. Simulating the discharge and ∇_{wt} responses separately

Fig. 7 shows the distribution of behavioural parameter values (from run_1) for both LU's over the sampled ranges listed in Table 2. Each column is associated with parameter ranges that meet one or more behavioural criteria using the multiple objectives identified in Table 3. Table 5 lists the number of behavioural simulations associated with each criteria.

Simulations meeting the behavioural criterion for discharge (Fig. 7 - column 1) show limited parameter sensitivity for the ranges sampled, only SZM and $\ln(T_0)$ from the HS_{LU} show any sensitivity, with only the $\ln(T_0)$ parameter constrained to its lower range from the initial sampling limits listed in Table 2. Table 5 also lists the large number (41% of the initial sample of 5.6million runs) of simulations that meet the behavioural threshold for the discharge criterion. Surprisingly almost no sensitivity is seen in the VB_{LU} parameters for simulations of discharge. Freer et al. (2003) reported a similar effect for Dynamic TOPMODEL simulations at PMRW where three LU's were identified. In that study, parameters for the VB_{LU} showed little sensitivity to discharge simulations. At PMRW this was attributed to a greater sensitivity of the HS_{LU} dynamics to wetting and drying cycles needed to capture the high seasonality in observed discharge. In both cases the insensitivity of the VB_{LU} could well be attributed to the relatively small areal extent of the LU (9% for PMRW and 12% for Maimai) as well as the product of landscape position and model conceptualisation. This suggests that for discharge simulations a simpler conceptual form for the VB_{LU} could be identified, potentially resulting in fewer, more easily identifiable parameters. Finally S_{max}, proven to be an important parameter for other applications of Dynamic TOPMODEL (i.e. Beven and Freer, 2001a) appears redundant here, perhaps reflecting the climatic and physical conditions found at Maimai (i.e. steep slopes, high transmissivities, consistently wet conditions). The need for a dynamic subsurface saturated zone that primarily controls wetting and drying cycles is not required for behavioural simulations. For simulations meeting the fuzzy criteria for both tensiometer sites independently

Table 5
Behavioural simulations for individual and combined acceptance criteria for the performance measures identified in Table 3 from both run_1 and run_2

Acceptability criteria	run_1 behavioural simulations[a]		run_2 behavioural simulations[b]		run_1 and run_2
	Total number	Sampling efficiency (%)	Total number	Sampling efficiency (%)	Sampling efficiency increase
Discharge only	2,327,664	41.56	1,016,325	84.69	2.0
NS ∇_{wt} only	196,591	3.51	118,519	9.87	2.8
P5 ∇_{wt} only	16,195	0.28	39,128	3.26	11.5
Discharge and NS ∇_{wt}	84,636	1.51	98,218	8.18	5.4
Discharge and *P5* ∇_{wt}	11,987	0.21	34,205	2.80	13.3
NS ∇_{wt} and *P5* ∇_{wt}	614	0.011	3,692	0.31	28.2
Discharge, NS and *P5* ∇_{wt}	419	0.007	3,184	0.26	37.1

[a] Total number of all simulations was 5,600,000.
[b] Total number of all simulations was 1,200,000.

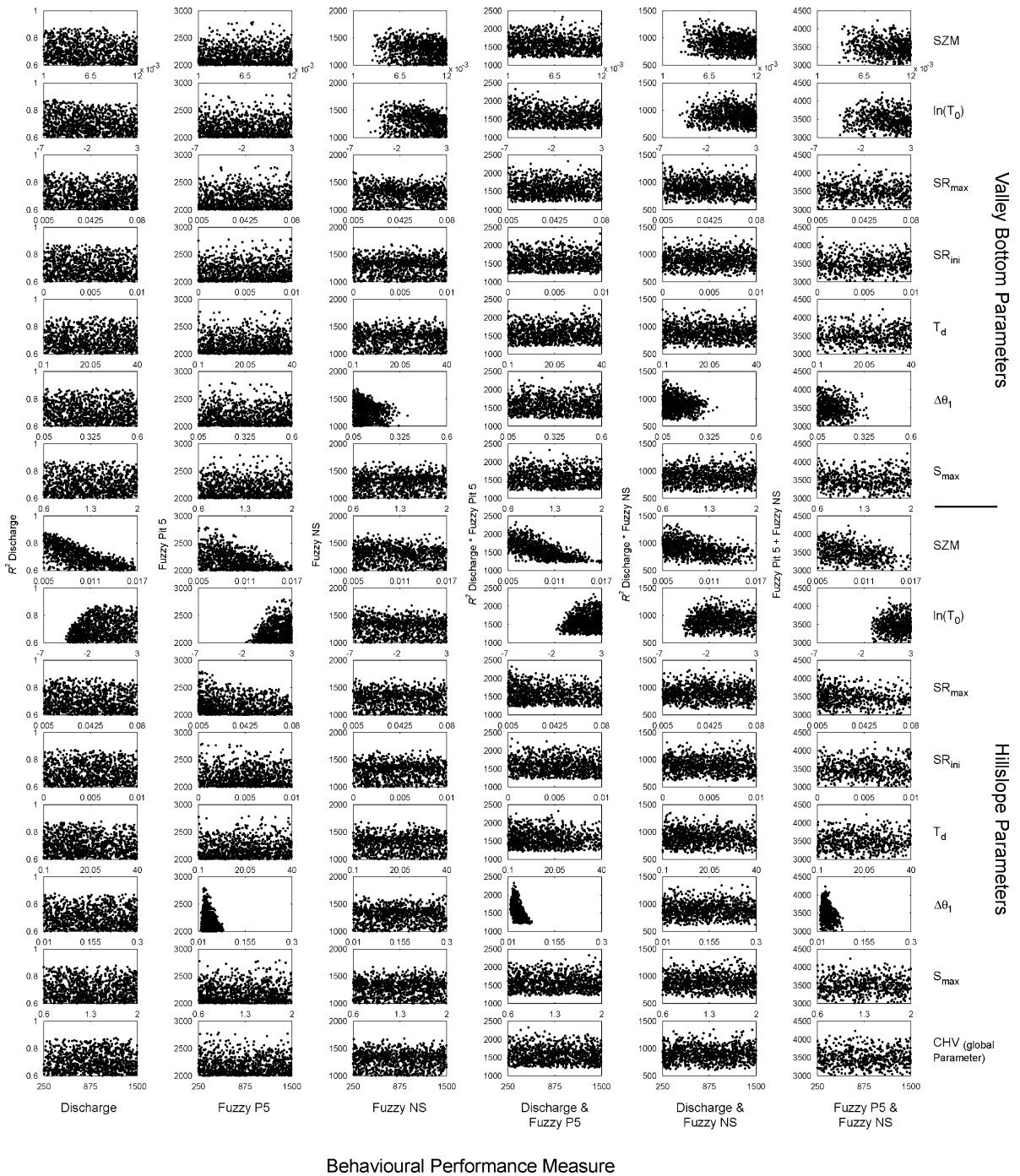

Fig. 7. Dotty plots of behavioural parameter distributions for both the VB_{LU} (rows1-7) and the HS_{LU} (rows 8–14) for the different performance measures (or combinations of measures) listed in Table 3. Each column distinguishes between the different performance measures or combinations of measures (plots show a random sample of up to 1,000 points from the total number of behavioural parameter sets listed in Table 4).

(see Table 3) there are different but somewhat consistent results with the discharge simulations (Fig. 7 columns 2 and 3 for the *P5* and NS sites respectfully).

For the *P5* site the HS_{LU} parameters *SZM* and ln (T_0) show similar distributions to the discharge simulations. However, $\Delta\theta_1$ is now highly sensitive in its lower range and SR_{max} also shows some sensitivity. The high sensitivity of $\Delta\theta_1$ should be expected, this parameter is one of the primary controls of the mean depth of the predicted ∇_{wt} within the model (the difference in the water content between saturation and field capacity), effectively acting as a simple scaling of the local moisture deficit. For this criterion the number of behavioural simulations is much reduced (see Table 5), and can be attributed to the high sensitivity of $\Delta\theta_1$ reported reducing the efficiency of the uniform sampling employed.

Comparing the number of behavioural simulations for the NS site with those for the *P5* site the latter produces a considerably greater number. This is directly reflected in the broader range of $\Delta\theta_1$ for the VB_{LU} that partly results from wider fuzzy limits in the observed ∇_{wt} series (especially at depth) shown in Fig. 4. What is surprising about the simulations meeting the NS behavioural criterion is how little sensitivity is observed within the HS_{LU}, especially given the proximity of this LU to the NS site (see Fig. 1b).

4.2. Meeting discharge and/or tensiometer criteria for more than one source of information

Parameter distributions from simulations that are behavioural for a combination of two PM criteria from Table 3 are shown in Fig. 7 columns 4–6 and for a combination of all PM in Fig. 8. To simply highlight the combined effect of the PM's to the parameter sensitivity the dotty plots shown in Fig. 7 are either a multiplicative combination of discharge and ∇_{wt} PM's (Fig. 7, column 4-5) or an additive combination of the combined NS and *P5* ∇_{wt} PM's (Fig. 7, column 6). Due to the insensitivity of the VB_{LU} for discharge, coupled with the similarity of the behavioural distributions for discharge and *P5* PM for the HS_{LU}, the combined behavioural PM distributions almost always reflect the PM sensitivity for the individual ∇_{wt} distributions previously shown in Fig. 7 (columns 2 and 3). Combining discharge with the NS and *P5* PM's further reduces the number of behavioural parameter sets (Table 5). However, only 3.8% of parameter sets are retained for a combined NS and *P5* PM from the maximum possible number of behavioural parameter sets for either of these two sites. This incompatibility of parameter distributions is the result of the general insensitivity of each LU's parameters to simulating the other LU's ∇_{wt} information. In combination the void space throughout the parametric hyperspace (i.e. the area of the parameter space where no behavioural simulations are found) increases rapidly due to the constraining of parameter ranges in both LU's, thus reducing sampling efficiencies (i.e. a reduction in the percentage of the total number of simulations that are behavioural).

Fig. 8 shows the marginal posterior likelihood weighted distributions of individual parameters as histograms, and the interaction of parameters both within and between LU's for the final behavioural parameter sets constrained using all three PM's from run_2 (having an efficiency of sampling of 0.26%, see Table 5). Parameter sensitivities are similar to those shown in Fig. 7 column 6 for the combined NS and *P5* PM's (note parameter ranges in Fig. 8 are consistent with the ranges listed in Table 4 for run_2). Although a number of parameters are sensitive across their individual ranges, the bi-variate plots of parameter interactions show that few correlation structures are clearly identified, especially for parameter interactions between LU's. This point is confirmed by the strength of the correlation co-efficients, where only $\Delta\theta_1$ and its relationship to SZM and ln (T_0) for both LU's have co-efficients above ± 0.25. More complex, non-linear and multi-dimensional structures may well exist, and will be reflected in the parameter *sets* that give behavioural PM's.

The behavioural simulations for all PM's identified in Table 5 and Fig. 8 were then used to determine the upper and lower possibility limits for the discharge, NS ∇_{wt} depths and *P5* ∇_{wt} depths, these results are presented in Fig. 9 (note that discharge is also plotted in log units in Fig. 9B). The results show that although the range of simulations generally envelop (or are within the range of) the different observations, this is not the case for all time steps, and for some periods there are significant departures. For discharge the results are encouraging, even when shown as log transformed flows (Fig. 9b.). Periods of rapid

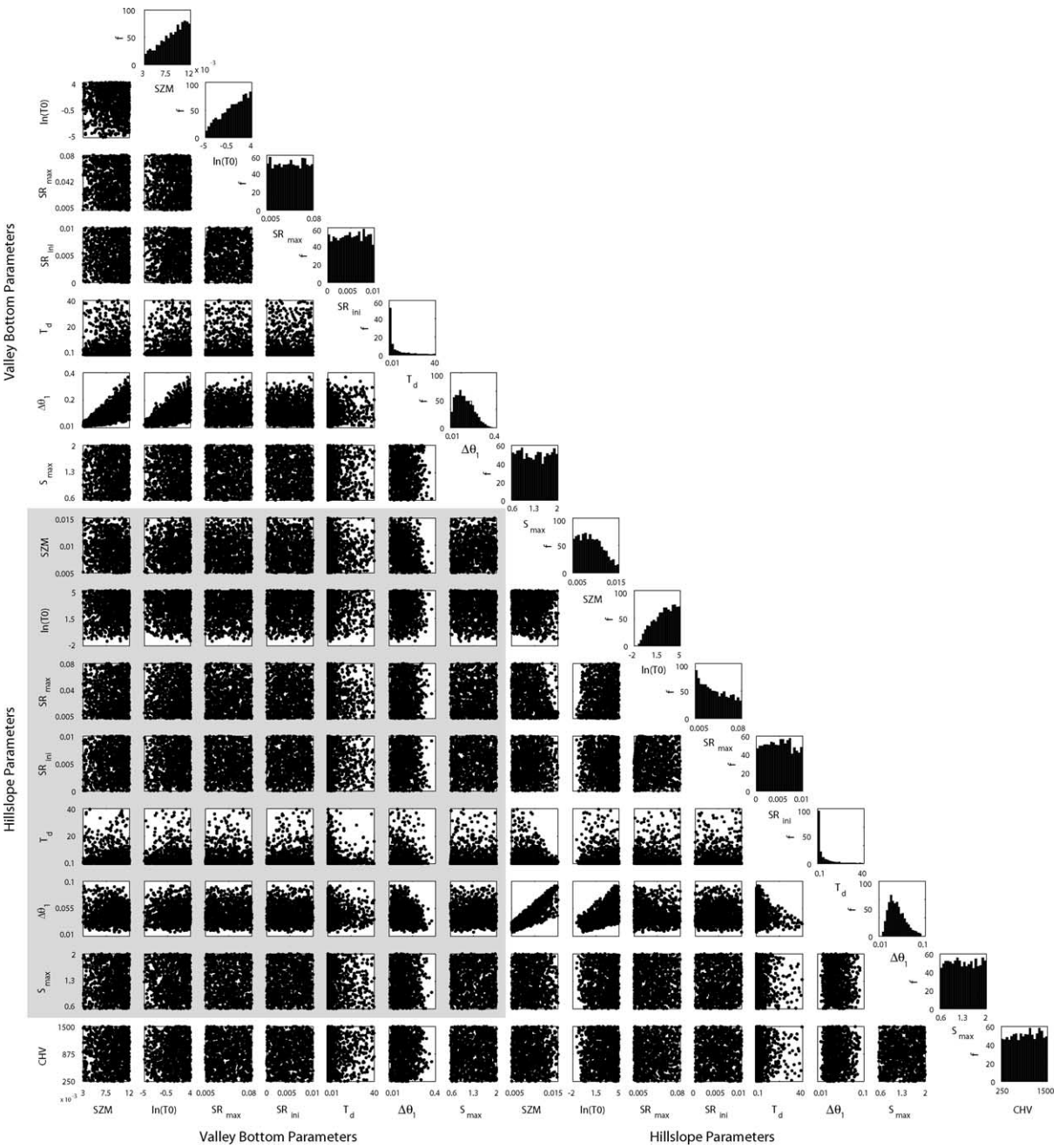

Fig. 8. Dotty plots and histograms of behavioural parameter distributions from run_2 for both the VB_{LU} and the HS_{LU} for parameter sets that were classed as behavioural for all three performance measures listed in Table 3. The main matrix of dotty plots shows the correlation between pairs of parameters within the same LU and between the HS_{LU} and VB_{LU} LU's (the greyed area). Each histogram shows the distribution of behavioural parameters within each parameter range (note the range limits are shown for the run_1 limits).

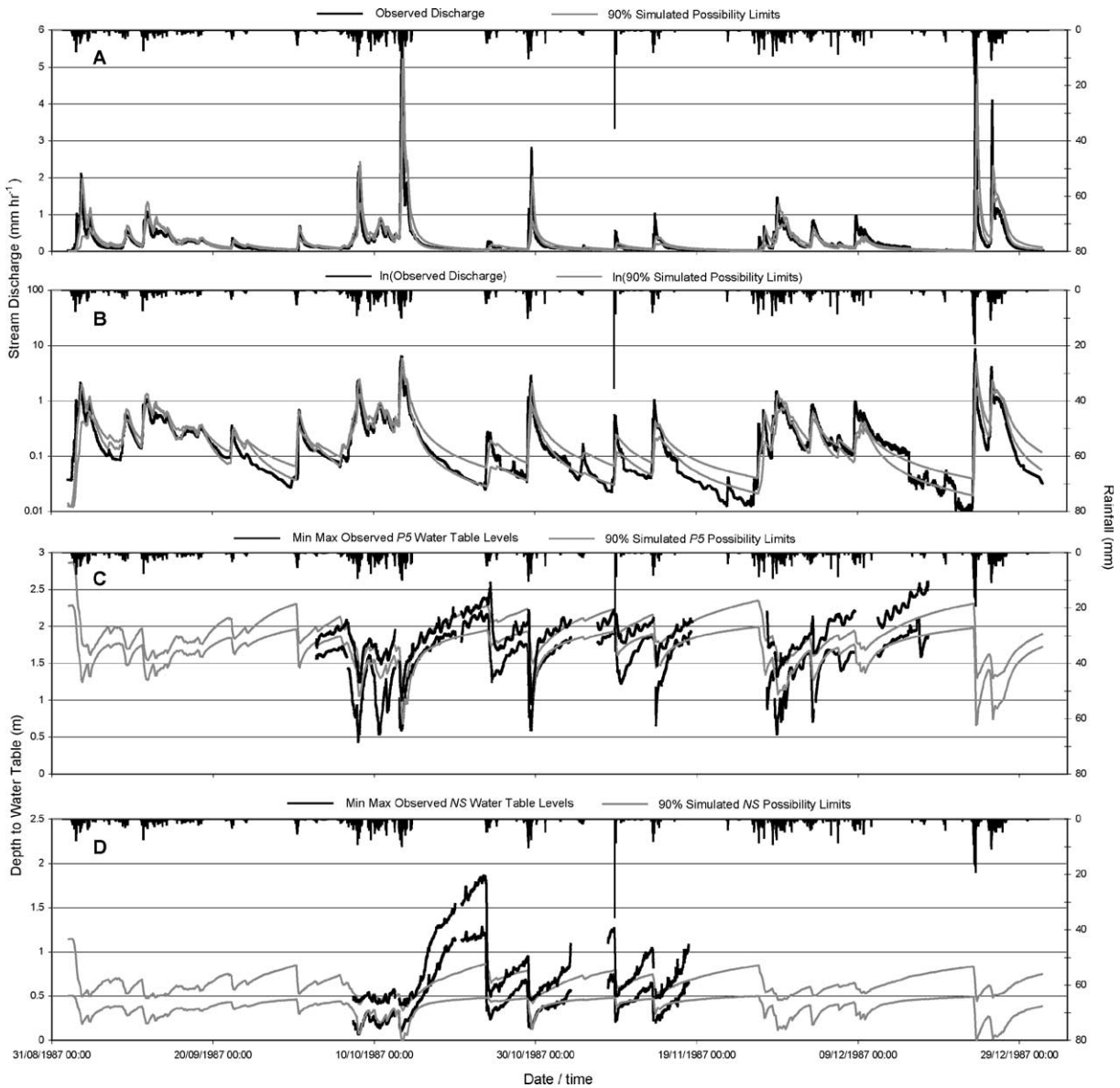

Fig. 9. GLUE Discharge, NS ∇_{wt} and *P5* ∇_{wt} updated behavioural possibility bounds for (A) Discharge, (B) ln (Discharge), (C) *P5* ∇_{wt} and (D) NS ∇_{wt} simulations.

fluctuations from a general recession form are likely to reflect observed data uncertainties not yet accounted for.

The *P5* simulations are within the range of the ∇_{wt} uncertainty limits for most of the study period. The exception to this is the period before the 29th October storm event where the distribution of simulated ∇_{wt} depths are deeper than those of the observed. This period is preceded by a considerable recession period (for Maimai) that may suggest even moderate wetting up sequences are not well represented in the model dynamics. Non-linearity in catchment response can be highlighted by the relationship between peak discharges and the maximum ∇_{wt} rise at the *P5* site. A consistent pattern is not apparent, where considerable differences in discharge peaks produce similar rises in

observed ∇_{wt} depths, in some cases smaller discharge peaks result in the highest ∇_{wt} rises.

The NS simulations show the most extensive departures from the range of ∇_{wt} observations, primarily during the recession period previously mentioned. This rapid increase in the observed ∇_{wt} depths (that seems to begin to be replicated at the end of the NS observations) may be systematic of local phenomena such as non-linearity in the storage-discharge relationship with the different soil horizons. However, this could also be the result of a breakdown in the relationship between the − ve matric potentials and height above ∇_{wt} at the NS site. Certainly McDonnell (1990) reported a bedrock depth of 0.5 m at the NS pit face, however, this local depth is highly variable (as noted by McDonnell, 1990) as identified by the 0.78 m tensiometer placement in Nest 1 (see Fig. 1(c)). Departures occur in the NS simulations during periods where + ve matric potential readings are observed, which suggest the rapidly increasing ∇_{wt} depths have some validity.

Finally the characteristics in the NS and *P5* simulations relate well to the variability in the parameter distributions for these LU's. For the HS_{LU} lower SZM and higher $\Delta\theta_1$ parameter distributions reflect the steeper and deeper *P5* ∇_{wt} recession characteristics. Previously Freer (1998), using the original form of TOPMODEL, identified these controlling parameters as the reason why the model was unable to simulate the ∇_{wt} responses at both sites using homogeneously applied catchment scale parameters.

4.3. Constraining model responses and the efficiency of sampling

For the different behavioural parameter sets identified in Table 5, Fig. 10 shows the distribution

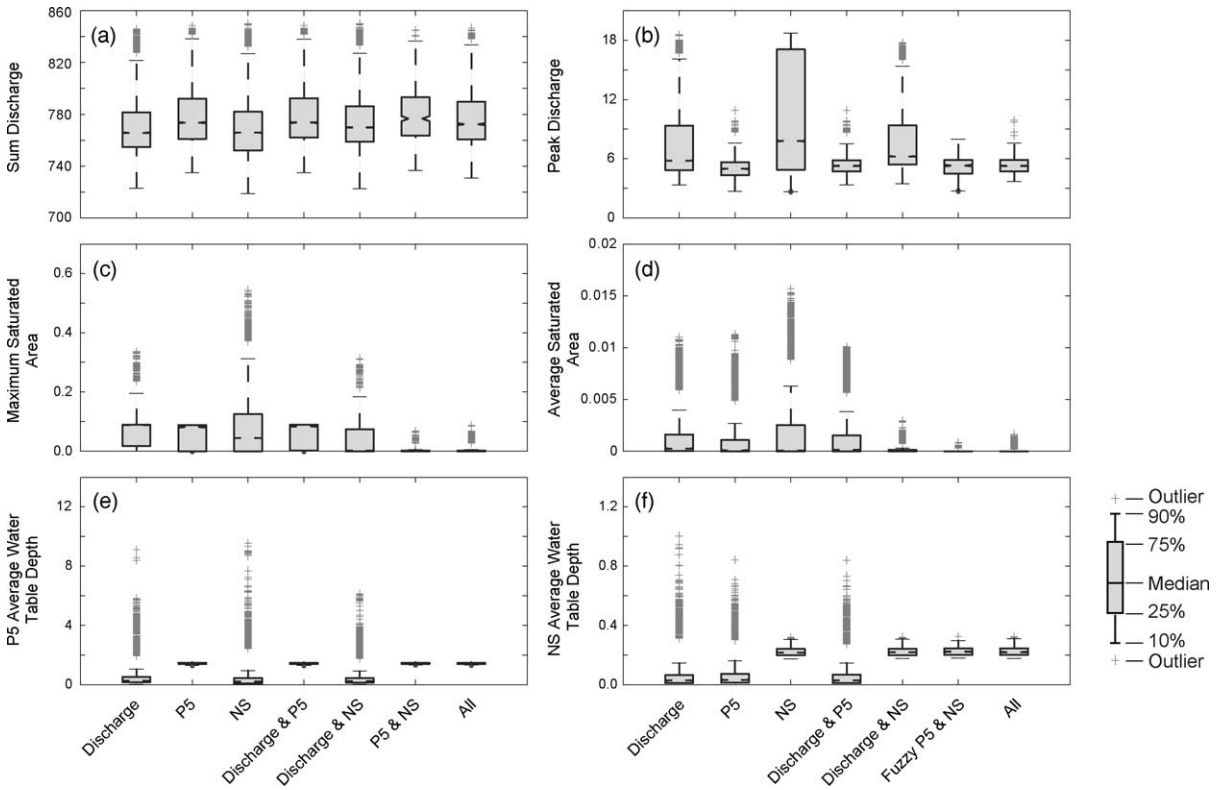

Fig. 10. Distributions of summary model responses for behavioural simulations using different PM's or combinations of PM's listed in Table 4. An outlier is a value that is more than 1.5 times the inter-quartile range away from the top or bottom of the box.

of a number of summary model responses calculated from each simulation run. Fig. 10 shows that the range of model behaviour can vary considerably between the different behavioural parameter sets (i.e. peak discharge). In nearly all cases (apart from Sum Discharge Fig. 10a where limits for this measure are generally consistent for all PM's) simulations conditioned using all the PM's show the smallest range of model behaviours. Treated individually, the *P5* PM constrains the model responses most; that this also occurs for the range of Peak Discharge responses is somewhat surprising. Perhaps this is indicative of the discriminatory power of the R^2 measure, the strength of which has been questioned in a number of recent studies (i.e. Gupta et al., 1998; Legates and McCabe, 1999; Freer et al., 2003). The average ∇_{wt} depth ranges for the *P5* and NS sites (Fig. 10e and f) identify why only a small proportion of simulations that are behavioural for one site are also behavioural for the other. The distributions of these average ∇_{wt} depths have very little overlap and must reflect a general inability to simulate the ∇_{wt} observations to an acceptable level.

Distributions of model responses for the NS PM, coupled with the lack of sensitivity in parameter distributions for the same PM shown in Fig. 8, suggest this PM has the least discriminatory power. This leads to output model responses that seem uncharacteristic of catchment behaviour (i.e. the high peak discharges and maximum saturated areas shown in Fig. 10b and c). Partly this is a product of the information content in the fuzzy NS ∇_{wt} observations, i.e. generally wider limits and lower amplitudes of responses compared to the *P5* data, but also this reflects the general insensitivity of this LU described in Section 4.1.

4.4. Can we improve the model structure and parameter representation?

The simulation results thus far presented have resulted in good simulations of the Maimai catchment discharge and ∇_{wt} responses. Where this has not been the case (i.e. the deeper ∇_{wt} recessions at the NS site) further data collection would be required to confirm the potential for variability at the model prediction scale. What is not clear from these results is whether additional data sets (i.e. more ∇_{wt} sites or the use of tracer data) would still maintain a compatible set of parameter estimates or lead to the rejection of all model simulations. Would each new observation site require a new set of parameter distributions and/or changes to the basic model structure, similar to that reported by Lamb et al. (1998)? An important question for modellers in this regard is how approximate can a model be and still retain an element of realism in predicting quantities and fluxes of interest. Even if the general structure of dynamic TOPMODEL is a reasonable approximation for the hydrological response at Maimai, model parameters are more heterogeneous in space than our definition of two LU's have characterised. The use of internal state data is desirable, but given the necessarily limited and local nature of the internal state data, would the predictions elsewhere in the catchment be strongly biased by this form of conditioning. Certainly the information pertaining to the characterisation of hydrological responses at Maimai used in this study are still limited. This is important as the effective gridscale uncertainties in the ∇_{wt} responses for both the NS and *P5* sites may well be greater than those currently identified. Given that ∇_{wt} was sampled at nine and 11 locations in the *P5* and NS sites, respectively, demonstrating significant variation across the gridcell, it would be reasonable to suppose that this sample reflects only part of the range actually present across the gridcell. A case therefore could be made for widening the fuzzy limits beyond the observed extreme points. We may, therefore, still be biasing our range of simulated behaviour due to poorly defined observational uncertainties. Perhaps what is more likely if additional observations were available is that each new site that is added to the constraining information (in this case ∇_{wt} information) will have characteristics that are in some way unique (Beven, 2000). Small to potentially large variations in local parameter distributions may be required to simulate such information. Observations from the NS and *P5* sites clearly show that the subsurface dynamics are different, the sites are clearly drawn from topographically distinct regions of the catchment, and that these differences have been reflected in the behavioural parameter distributions for the two LU's.

The general hydrological regime at Maimai lends itself to the primary assumptions embedded in the dynamic TOPMODEL framework. However,

the perceptual model of the subsurface flow processes at Maimai includes mechanisms that are not explicitly accounted for in the model structure, i.e. horizontal preferential macropore flowpaths, vertical bypassing to depth, variable porosity values in the organic and mineral soil horizons (see Mosley, 1979; McDonnell, 1990; McGlynn et al., 2002). With this in mind our modelling results are surprisingly good for the ∇_{wt} dynamics. That parameter estimates and model responses seem to make physical sense with observational data from Maimai is also encouraging. For example Pearce et al. (1986) suggest maximum saturated areas at Maimai are in the region of 4–7%, comparing well with the results presented in Fig. 10c for the simulations constrained by all the PM's.

However, insensitivity in many parameters and a lack of interaction between parameters suggests the conceptual framework of the model for Maimai catchment could be improved, if only to reduce the redundancy of certain parameters. Would it be possible with increased information to identify for the local place (i.e. a LU) a subset of parameters that characterises the uniqueness of that place? In this case a combination of SZM, $\ln(T_0)$ and $\Delta\theta_1$ would seem appropriate for characterising the ∇_{wt} dynamics, thereby reducing the total number of parameters that need to be uniquely defined for each LU. Or would new subsets of parameters and model structure components be required for the inclusion of each new place and/or each new type of observed data?

5. Conclusions

This paper presents an approach to assessing the internal accuracy of dynamic TOPMODEL, recognising that internal state data available to the modeller are inherently uncertain. The model was applied to the Maimai M8 catchment in New Zealand, and was refined by using two topographically-distinct LU's ('Hillslope' and 'Valley Bottom') with separate parameterisations. For each location, a nest of tensiometers located within an area more commensurate with the model gridscale provided a distribution of matric potentials, which were then converted to water table depth. These depths were used together with rainfall–runoff data to constrain the model using the Generalised likelihood uncertainty estimation methodology.

The use of localised data to assess model performance presents particular problems to the modeller. Unlike aggregated components such as river discharge, water table responses more strongly reflect localised and smaller-scale characteristics of catchment processes, and this is clearly demonstrated in the variability shown in the tensiometer readings within the area of one gridcell. Although tensiometers were positioned to avoid cracks and voids in the soils where these were visibly identifiable, the effects of heterogeneity of soil characteristics and flow pathways, such as macropores and soil structure, cannot be avoided. When these locally conditioned data are used to constrain the model, the model structure and parameterisation may then be biased towards these local structures which may not be the 'best' representation of the average response of the catchment, or indeed at a scale comparable to the model gridscale, this being the smallest spatial scale of hydrological process representation in the model. As increasing numbers of these local criteria are enforced, the model will be unable to incorporate the complexity of local observations and the danger is that all simulations are rejected as non-behavioural or that increasing numbers of local parameters must be used.

In an attempt to respond to these problems, fuzzy performance measures of ∇_{wt} predictions were used. These allow the modeller to include knowledge of errors in the internal state data presented and are not so constrained by the need for a particular error structure throughout the data series. The authors wish to note that the variability of the tensiometer readings in time and space are clearly not the only source of observed data uncertainty driving our model simulations. Similar techniques could also be applied to the rainfall, evaporation and discharge observations.

In this study a trapezoidal form of fuzzy measure was used to incorporate knowledge of the distribution of water table depths at the two test sites. However, despite the use of fuzzy measures to relax the assumptions of these criteria, the retention rate for parameter sets picked using the more efficient constrained sampling ranges in run_2 dropped from 84.69% (discharge only) to 0.26% when using all three performance measures. This sparseness of

behavioural parameter sets suggests both a complex structure within the parameter space, and individuality of water table depths internally to the catchment. Intuition suggests that the NS water table data should be less location dependent and more representative of the overall ∇_{wt} dynamics of the catchment than the *P5*data. The NS site integrates a greater catchment drainage area and therefore proportionally this site is more likely to be representative of the overall catchment dynamics that characterise streamflow response. This was borne out by the higher sampling efficiency when using internal data only from the NSsite as oppose to only the *P5*site.

This study has demonstrated that when using dynamic TOPMODEL to make predictions about internal catchment dynamics, it is not sufficient to condition the model using aggregate performance data such as discharge. The uniqueness of place demonstrated at and within each gridcell area is not reflected in such integrated measures; and therefore internal state data are required to enable model calibration if the model is to provide a more accurate representation of the catchment processes (see also Seibert and McDonnell, 2002). Such evaluations will become ever more pertinent as internal state data become more readily available through improved measurement and remote-sensing techniques.

The use of fuzzy measures for evaluating hydrological models is a powerful and flexible tool in situations where there is no or incomplete knowledge of the error structure and local variability of the phenomenon. The exact form of the measure can be designed to reflect uncertainties particular to the modelling situation. Equally, this very adaptability means that consistent, global rules for function definition cannot be specified; instead the user must be clear as to the motivation that underlies the chosen measure, as was the aim in this paper. The challenge will be to develop methods that are both realistic and flexible about the nature of such errors but still maintain a sound scientific justification and/or evaluation of the error terms.

Acknowledgements

We thank Stefan Uhlenbrook, Rodger Grayson, Ralf Ludwig and one anonymous reviewer for their valuable comments. This research was partly funded by NER/L/S/2001/00658 and NSF EAR 0196381.

References

Anderton, S., Latron, M., Gallart, F., 2002a. Sensitivity analysis and multi-response, multi-criteria evaluation of a physically based distributed model. Hydrological Processes 16 (2), 333–353.

Anderton, S.P., Latron, J., White, S.M., Llorens, P., Gallart, F., Salvany, C., O'Connell, P.E., 2002b. Internal evaluation of a physically-based distributed model using data from a Mediterranean mountain catchment. Hydrology and Earth System Sciences 6 (1), 67–83.

Aronica, G., Bates, P.D., Horritt, M.S., 2002. Assessing the uncertainty in distributed model predictions using observed binary pattern information within GLUE. Hydrological Processes 16 (10), 2001–2016.

Barling, R.D., Moore, I.D., Grayson, R.B., 1994. A quasi–dynamic wetness index for characterizing the spatial-distribution of zones of surface saturation and soil–water content. Water Resources Research 30 (4), 1029–1044.

Bathurst, J.C., O'Connell, P.E., 1992. Future of distributed modelling—the Systeme-Hydrologique-Europeen. Hydrological Processes 6 (3), 265–277.

Beck, M.B., Halfon, E., 1991. Uncertainty, identifiability and the propagation of prediction errors—a case-study of Lake-Ontario. Journal of Forecasting 10 (1-2), 135–161.

Beven, K.J., 1989. Changing ideas in hydrology—the case of physically-based models. Journal of Hydrology 105 (1-2), 157–172.

Beven, K.J., 1996. Equifinality and uncertainty in geomorphological modelling. The Scientific Nature of Geomorphology, Proceedings of the 27th Binghampton Symposium in Geomorphology held 27–29 September, Binghampton,.

Beven, K.J., 1997. TOPMODEL: a critique. Hydrological Processes 11 (9), 1069–1085.

Beven, K.J., 2000. Uniqueness of place and process representations in hydrological modelling. Hydrology and Earth System Sciences 4 (2), 203–213.

Beven, K.J., 2002. Towards a coherent philosphy for modelling the environment. Proceedings of the Royal Society London A 458, 2465–2484.

Beven, K.J., Freer, J., 2001a. A dynamic TOPMODEL. Hydrological Processes 15 (10), 1993–2011.

Beven, K.J., Freer, J., 2001b. Equifinality, data assimilation, and uncertainty estimation in mechanistic modelling of complex environmental systems using the GLUE methodology. Journal of Hydrology 249 (1–4), 11–29.

Beven, K.J., Kirkby, M.J., 1979. A physically based, variable contributing area model of basin hydrology. Hydrological Sciences Bulletin–Bulletin Des Sciences Hydrologiques 24 (1), 43–69.

Blazkova, S., Beven, K.J., Kulasova, A., 2002. On constraining TOPMODEL hydrograph simulations using partial saturated area information. Hydrological Processes 16 (2), 441–458.

Bloschl, G., Gutknecht, D., Kirnbauer, R., 1992. On the evaluation of distributed hydrologic models, Advances in Distributed Hydrology (workshop), Seriate (Bergamo), Italy, 25–26th June.

Burt, T.P., Butcher, D.P., 1985. Topographic controls of soil moisture distributions. Journal of Soil Science 36, 469–486.

Burt, T.P., Butcher, D.P., 1986. Development of topographic indices for use in semi-distributed hillslope runoff models. Z. Geomorphological 58, 1–19.

Butcher, D.P., 1985. Field verification of topographic indicies for use in a hillslope runoff model. Unpublished PhD Thesis, Huddersfield Polytechnic, Huddersfield.

Franks, S.W., Gineste, P., Beven, K.J., Merot, P., 1998. On constraining the predictions of a distributed moder: the incorporation of fuzzy estimates of saturated areas into the calibration process. Water Resources Research 34 (4), 787–797.

Freer, J.E., 1998. Uncertainty and Calibration of Conceptual Rainfall Runoff Models. Unpublished PhD Thesis, Lancaster University, Lancaster, pp. 282.

Freer, J., Beven, K., Ambroise, B., 1996. Bayesian estimation of uncertainty in runoff prediction and the value of data: an application of the GLUE approach. Water Resources Research 32 (7), 2161–2173.

Freer, J.E., Beven, K.J., Peters, N.E., 2003. Multivariate seasonal period model rejection within the generalised likelihood uncertainty estimation procedure. In: Duan, Q., Gupta, H., Sorooshian, S., Rousseau, A.N., Turcotte, R. (Eds.), Calibration of watershed models. AGU, Water Science and Application Series, Washington, pp. 346.

Grayson, R., Bloschl, G., 2000. Spatial patterns in catchment hydrology: observations and modelling. Cambridge University Press, Cambridge, pp. 404.

Grayson, R.B., Moore, I.D., McMahon, T.A., 1992. Physically Based Hydrologic Modelling 2. Is the Concept Realistic. Water Resources Research 28 (10), 2659–2666.

de Grosbois, E., Hooper, R.P., Christophersen, N., 1988. A multisignal automatic calibration methodology for hydrochemical models—a case-study of the Birkenes model. Water Resources Research 24 (8), 1299–1307.

Guntner, A., Uhlenbrook, S., Seibert, J., Leibundgut, C., 1999. Multi-criterial validation of TOPMODEL in a mountainous catchment. Hydrological Processes 13 (11), 1603–1620.

Gupta, H.V., Sorooshian, S., Yapo, P.O., 1998. Toward improved calibration of hydrologic models: multiple and noncommensurable measures of information. Water Resources Research 34 (4), 751–763.

Hewlett, J.D., Hibbert, A.R., 1967. Factors affecting the response of small watersheds to precipitation in humid areas, International Symposium on Forest Hydrology,.

Hooper, R.P., Stone, A., Christophersen, N., de Grosbois, E., Seip, H.M., 1988. Assessing the Birkenes model of stream acidification using a multisignal calibration methodology. Water Resources Research 24 (8), 1308–1316.

Kirkby, M., 1975. In: Peel, R., Chisholm, M., Haggett, P. (Eds.), Hydrograph Modelling Strategies, Processes in Physical and Human Geography, Heinemann, London, pp. 69–90.

Koide, S., Wheater, H.S., 1992. Subsurface Flow Simulation of a Small Plot at Loch-Chon, Scotland. Hydrological Processes 6 (3), 299–326.

Kosugi, K., Inoue, M., 2002. Estimation of hydraulic properties of vertically heterogeneous forest soil from transient matric pressure data. Water Resources Research 38 (12) art. no.-1322.

Kuczera, G., 1983. Improved parameter inference in catchment models. 2. Combining different kinds of hydrologic data and testing their compatibility. Water Resources Research 19 (5), 1163–1172.

Kuczera, G., Mroczkowski, M., 1998. Assessment of hydrologic parameter uncertainty and the worth of multiresponse data. Water Resources Research 34 (6), 1481–1489.

Lamb, R., Beven, K.J., Myrabo, S., 1997. Discharge and water table predictions using a generalized TOPMODEL formulation. Hydrological Processes 11 (9), 1145–1167.

Lamb, R., Beven, K.J., Myrabo, S., 1998. Use of spatially distributed water table observations to constrain uncertainty in a rainfall–runoff model. Advances in Water Resources 22 (4), 305–317.

Legates, D.R., McCabe, G.J. Jr., 1999. Evaluating the use of goodness-of-fit measures in hydrologic and hydroclimatic model validation. Water Resources Research 35 (1), 233–241.

McDonnell, J.J., 1989. The age, origin and pathway of subsuirface stormflow in a steep, humid headwater catchment. Unpublished PhD Thesis, University of Canterbury, Christchurch, NZ, 270 pp.

McDonnell, J.J., 1990. A rationale for old water discharge through macropores in a steep, humid catchment. Water Resources Research 26 (11), 2821–2832.

McDonnell, J.J., 1993. Technical notes: electronic versus fluid multiplexing in recording tensiometer systems. ASAE Publication 36 (2), 459–462.

McDonnell, J.J., Stewart, M.K., Owens, I.F., 1991. Effect of catchment-scale subsurface mixing on stream isotopic response. Water Resources Research 27 (12), 3065–3073.

McGlynn, B.L., McDonnell, J.J., 2003. Role of discrete landscape units in controlling catchment dissolved organic carbon dynamics. Water Resources Research 39 (4) art. no.-1090.

McGlynn, B.L., McDonnell, J.J., Brammer, D.D., 2002. A review of the evolving perceptual model of hillslope flowpaths at the Maimai catchments. New Zealand. Journal of Hydrology 257 (1-4), 1–26.

Mew, G., Webb, T.H., Ross, C.W., Adams, J., 1975. Soils of Ignangahua depression, South Island, New Zealand, 17. New Zealand Soil Survey, Christchurch.

Mosley, M.P., 1979. Streamflow generation in a forested watershed, New Zealand. Water Resources Research 15 (4), 795–806.

Motovilov, Y., Gottschalk, L., Engeland, K., Rodhe, A., 1999. Validation of a distributed hydrological model against spatial observations. Agricultural and Forest Meteorology 98-99, 257–277.

Mroczkowski, M., Raper, G.P., Kuczera, G., 1997. The quest for more powerful validation of conceptual catchment models. Water Resources Research 33 (10), 2325–2335.

Pearce, A.J., McKercher, A.I., 1979. Upstream generation of storm runoff. In: Murray, D.L.A., (Ed.), Physical Hydrology—New Zealand Experience, New Zealand Hydrological Society, Wellington, pp. 165–192.

Pearce, A.J., Stewart, M.K., Sklash, M.G., 1986. Storm runoff generation in humid headwater catchments. 1. Where does the water come from. Water Resources Research 22 (8), 1263–1272.

Peters, N.E., Freer, J.E., Beven, K.J., 2001. Modeling hydrologic responses in a small forested watershed by a new dynamic TOPMODEL (Panola Mountain, Georgia, USA). In: Uhlenbrook, S., Leibundgut, C., McDonnell, J.J. (Eds.), Runoff Generation and Implications for River Basin Modeling, Freiburger Schriften zur Hydrologie, Band 13, Frieburg, pp. 318–325.

Peters, N.E., Freer, J., Beven, K.J., 2003. Modeling hydrologic responses in a small forested catchment (Panola Mountain, Georgia, USA)—a comparison of the original and a new dynamic TOPMODEL. Hydrological Processes 17 (3), 345–362.

Quinn, P.F., Beven, K.J., Chevallier, P., Planchon, O., 1991. The prediction of hillslope flow patterns for distributed hydrological modelling using digital terrain models. Hydrological Processes 5, 59–59.

Rezaur, R.B., Rahardjo, H., Leong, E.C., 2002. Spatial and temporal variability of pore-water pressures in residual soil slopes in a tropical climate. Earth Surface Processes and Landforms 27 (3), 317–338.

Ross, T.J., 1995. Fuzzy Logic with Engineering Applications. McGraw-Hill, New York, pp. 600.

Rowe, L.K., 1979. Rainfall interception by a Beech-Podocarp-Hardwood forest near Reefton, North Westland, New Zealand. Journal of Hydrology (NZ) 18 (2), 63–87.

Rowe, L.K., Pearce, A.J., O'Loughlin, C.L., 1994. Hydrology and Related Changes after Harvesting Native Forest Catchments and Establishing Pinus-Radiata Plantations.1. Introduction to Study. Hydrological Processes 8 (3), 263–279.

Seibert, J., McDonnell, J.J., 2002. On the dialog between experimentalist and modeler in catchment hydrology: use of soft data for multicriteria model calibration. Water Resources Research 38 (11) art. no.-1241.

Sherlock, M.D., Chappell, N.A., McDonnell, J.J., 2000. Effects of experimental uncertainty on the calculation of hillslope flow paths. Hydrological Processes 14 (14), 2457–2471.

Sklash, M.G., 1990. Environmental isotope studies of storm and snowmelt runoff generation. In: Anderson, M.G.B., (Ed.), Process Studies in Hillslope Hydrology, Wiley, New York, pp. 401–435.

Sorooshian, S., Gupta, V.K., 1985. The analysis of structural identifiability—theory and application to conceptual rainfall–runoff models. Water Resources Research 21 (4), 487–495.

Stephenson, G.R., Freeze, R.A., 1974. Mathematical simulation of subsurface flow contributions to snowmelt runoff, Reynolds Creek watershed, Idaho. Water Resources Research 10 (2), 284–298.

Thiemann, M., Trosset, M., Gupta, H., Sorooshian, S., 2001. Bayesian recursive parameter estimation for hydrologic models. Water Resources Research 37 (10), 2521–2535.

Torres, R., Alexander, L.J., 2002. Intensity-duration effects on drainage: Column experiments at near-zero pressure head. Water Resources Research 38 (11) art. no.-1240.

Torres, R., Dietrich, W.E., Montgomery, D.R., Anderson, S.P., Loague, K., 1998. Unsaturated zone processes and the hydrologic response of a steep, unchanneled catchment. Water Resources Research 34 (8), 1865–1879.

Troch, P.A., Mancini, M., Paniconi, C., Wood, E.F., 1993. Evaluation of a distributed catchment scale water-balance model. Water Resources Research 29 (6), 1805–1817.

Uchida, T., Kosugi, K., Mizuyama, T., 2001. Effects of pipeflow on hydrological process and its relation to landslide: a review of pipeflow studies in forested headwater catchments. Hydrological Processes 15 (11), 2151–2174.

Uhlenbrook, S., Leibundgut, C., 2002. Process-oriented catchment modelling and multiple-response validation. Hydrological Processes 16 (2), 423–440.

Vertessy, R.A., Elsenbeer, H., 1999. Distributed modelling of storm flow generation in an Amazonian rain forest catchment: effects of model parameterization. Water Resources Research 35 (7), 2173–2187.

Wagener, T., Boyle, D.P., Lees, M.J., Wheater, H.S., Gupta, H.V., Sorooshian, S., 2001. A framework for development and application of hydrological models. Hydrology and Earth System Sciences 5 (1), 13–26.

Webster, J., 1977. The Hydrological Properties of the Forest Floor under Beech-Podocarp-Hardwood forest, North Westland. Unpublished PhD Thesis Thesis, Christchurch University, Canterbury, New Zealand.

Wigmosta, M.S., Lettenmaier, D.P., 1999. A comparison of simplified methods for routing topographically driven subsurface flow. Water Resources Research 35 (1), 255–264.